Role of molecular photodissociation in ultrafast laser surgery

Jenny Wang[a], Georg Schuele[b], Phil Huie[c], Daniel V. Palanker[c,d]
[a]Department of Applied Physics, Stanford University, 452 Lomita Mall, Stanford, CA 94305
[b]Abbott Medical Optics, 1310 Moffett Park Drive, Sunnyvale, CA 94089; [c]Department of Ophthalmology, Stanford University, 452 Lomita Mall, Stanford, CA 94305; [d]Hansen Experimental Physics Laboratory, 452 Lomita Mall, Stanford, CA 94305

ABSTRACT

Transparent ocular tissues such as cornea and crystalline lens can be precisely ablated or dissected using ultrafast ultraviolet, visible, and infrared lasers. In refractive or cataract surgery, cutting of the cornea, lens and lens capsule is typically produced by dielectric breakdown in the focus of a short-pulse laser which results in explosive vaporization of the interstitial water and mechanically ruptures the surrounding tissue. Here, we report that tissue can also be disrupted below the threshold of bubble appearance using 400 nm femtosecond pulses with minimal mechanical damage.

Using gel electrophoresis and liquid chromatography/mass spectrometry, we assessed photodissociation of proteins and polypeptides by 400 nm femtosecond pulses both below and above the cavitation bubble threshold. Negligible protein dissociation was observed with 800 nm femtosecond lasers even above the threshold of dielectric breakdown. Scanning electron microscopy of the cut edges in porcine lens capsule demonstrated that plasma-mediated cutting results in the formation of grooves. Below the cavitation bubble threshold, however, precise cutting could still be produced with 400 nm femtosecond pulses, possibly due to molecular photodissociation of the tissue structural proteins.

Keywords: ultrafast laser, laser-tissue interaction, cataract surgery, refractive surgery, protein, photodissociation, photofragmentation, photochemical

1. INTRODUCTION

Lasers are widely used in ocular surgery due to improved precision and reproducibility of the outcomes, compared to manual techniques. Current applications include corneal ablation by excimer lasers in refractive surgery[1], corneal dissection by femtosecond lasers in LASIK[2] or keratoplasty[3], as well as dissection of the lens and lens capsule in cataract surgery[4,5]. Basic research into laser-tissue interaction mechanisms[6,7] has helped to introduce new lasers such as 355 nm sub-nanosecond laser[8] or 1650 nm femtosecond laser[9] to corneal flap-cutting or new applications for currently used femtosecond lasers such as refractive index shaping[10]. In this study, we look at the interactions of the femtosecond pulses of Ti:Sapphire laser with lens capsule, and compare the quality of cuts produced by two wavelengths: 400 and 800 nm. The 400 nm femtosecond laser produces much smoother cuts and below the bubbles appearance. To understand this, we explore photodissociation of the proteins and polypeptides exposed to 400 and 800nm radiation.

2. METHODS

2.1 Femtosecond Laser system

A Ti:Sapphire oscillator (Tsunami, Spectra-Physics) was used to seed a Nd:YLF pumped (Merlin, Spectra-Physics) Ti:Sapphire regenerative amplifier system (Spitfire, Spectra-Physics) which generated 800 nm, 150 femtosecond pulses at 1 kHz. 400 nm pulses were produced via second harmonic generation (SHG) with a beta barium borate (BBO) crystal where needed. Several optical configurations were used in different parts of this experiment.

For lens capsule cutting at 400 nm wavelenght, two lenses in a Keplerian telescope configuration were used to expand the beam prior to the delivery through a 10X microscope objective (Olympus Plan-FL). The laser beam under-filled the objective for a NA of 0.1. Within the telescope, a half-waveplate and BBO crystal were used for SHG, and attenuation of the 400 nm was obtained by rotating the polarization out of optimal phase-matching. Two harmonic separator mirrors

(CVI Melles Griot) were used to select 400 nm and reject 800 nm wavelength. A co-aligned He-Ne laser and camera were used to position the lens sample at the proper focus. The sample stage was moved during laser cutting by two linear translation motors (Motor Mike, Oriel) driven by a custom LabView (National Instruments) program. Due to motor speed limitations, larger lateral spot spacing was obtained by dividing the laser repetition rate down to 100 Hz. Spacing could be varied between 0.1 μm to 2 μm. Vertical steps were created after each complete horizontal scan and varied between 4 and 10 μm. Pulse energy was measured with a power meter (PE9, Ophir Optronics), and ranged from 20 to 2000 nJ.

For lens capsule cutting with 800 nm wavelength, a similar setup was used. The SHG crystal was removed and a polarizing beam splitter was used instead to serve as an attenuator. Silver mirrors replaced the harmonic separators for steering the beam into the 10x objective at the same NA of 0.1. During cutting, pulse energy varied from 0.3 to 2 μJ, lateral spacing varied from 0.1 μm to 2 μm. Vertical steps were created after each complete horizontal scan and varied between 4 and 10 μm.

For protein and polypeptide photodissociation experiments, the setup was simplified by removing the telescope (for 800 nm) or converting to a relay (for 400 nm), and replacing the 10x objective with a singlet (f = 200 mm) for NA of 0.014. A scanning mirror (Optics in Motion) was used to scan the loosely focused beam through the protein or polypeptide solution that rested on a microscope slide. The scanning mirror was controlled via custom LabView (National Instruments) program to scan over the entire area of the fluid sample for the desired number of scans.

2.2 Lens capsule cutting

Pig eyes (First Vision Tech, Sunnyvale, Texas) were obtained from an abattoir and shipped overnight on ice. For 400 nm and 800 nm laser cutting, lenses were carefully extracted from the eye without puncturing the lens capsule, and stored in balanced salt solution (BSS) at 4°C until use. Lenses were used within 48 hours of extraction. During laser cutting, lenses were held in a plastic sample holder with a saline reservoir beneath to reduce drying. The top surface of the lens capsule was exposed to air during cutting of a straight line between 2 and 4 mm of lenth. For 1030 nm cutting, only the cornea was removed prior to laser capsulotomy using a Catalys (Abbott Medical Optics) system. After laser cutting in all cases, the anterior lens capsule containing the laser cut edges was removed from the lens, pinned to dental wax, and fixed in 1.25% gluteraldehyde. This helped prevent extruding lens material or folding during processing from obscuring the cut edge. After a minimum of 24 hours of fixation at room temperature, samples were processed as follows: 0.1 M sodium cacodylate rinse (30 min), Osmium Tetraoxide post-fixation (1 hr), 30% ethanol, 50% ethanol, 70% ethanol, 90% ethanol, 2 x 100% ethanol (20 min each). Samples were then critical point dried and sputter coated with 10 nm of Au/Pd before imaging by SEM (Hitachi S-3400N VP-SEM)

2.3 Excimer Laser System

ArF Excimer Laser (OPTex, Lambda Physik) producing 193 nm, 8 ns pulses was used to irradiate protein and polypeptide solution for photodissociation experiments. A diverging CaF_2 lens (f = 75 mm) was used to expand the beam area to cover the sample volume and an iris was used to define the irradiation area. The sample liquid was sandwiched between two quartz silica windows spaced with #1.5 coverslips. The incident pulse energy was measured with a pyroelectric energy sensor (PE-25BB, Ophir Optronics) and converted into fluence. For protein irradiation, a constant total energy of 20.6 mJ was delivered to the sample, while varying the pulse energy and total number of pulses to assess nonlinearity of the photodissociation effect. For HPLC analysis of polypeptide, pulse energy was kept constant, while the number of pulses was varied to observe the breakdown of the original polypeptide and accumulation of the breakdown products.

2.4 Protein breakdown analysis

Bovine serum albumin (BSA) was used as a common soluble protein of definite length (583 amino acids, 66.5 kDa) that could be analyzed after laser irradiation with gel electrophoresis. BSA was dissolved in water to a concentration of 1 mg/mL and irradiated by the different lasers described above. After irradiation, 10 μL was collected and processed for

gel electrophoresis using the Criterion XT system (Bio-Rad) according to manufacturer's protocol. For each gel, a control sample was placed on the sample surface but not irradiated. The gel was stained with Coomassie Blue R-250 for 1 hr and destained (40% Methanol, 10% Acetic acid) until background gel was clear.

Gels were placed on a lightbox and images were captured with a digital camera and analyzed in ImageJ with the Gel Analysis tool. The intact protein peak was measured for the control and laser-irradiated samples.

2.5 Polypeptide breakdown

A short, water-soluble, commercially available polypeptide was chosen to observe laser breakdown products using high performance liquid chromatography/mass spectrometry (HPLC/MS) with the sequence Trp-His-Trp-Leu-Gln-Leu (WHWLQL) with 882 MW. The polypeptide was dissolved in water and diluted to 0.1 mg/mL for laser irradiation. After irradiation, 5 μL were collected and analyzed using a Waters 2795 HPLC with Micromass ZQ single quadrupole MS (Vincent Coates Foundation Mass Spectrometry Laboratory). Mass spectrogram data was analyzed using MassLynx (Waters Corp.) software.

2.6 Bubble thresholds

Thresholds of the bubble formation were measured in solutions with different concentrations of BSA for 400 nm and 800 nm using a pressure transducer (VP-1093, CTS Valpey Corporation). Signals were processed through a pre-amplifier (SRS560, Stanford Research Systems) and viewed on an oscilloscope to determine bubble formation.

3. RESULTS

3.1 Lens capsule cutting

Porcine lens capsule were cut with 400 nm and 800 nm femtosecond laser using an initial spot spacing of 2 μm laterally and 10 μm vertically. Both beams were focused with NA of 0.1. Pulse energy was decreased until we found the minimum needed to cut through the lens capsule at this spot density. This was 0.75 μJ for 800 nm and 0.25 μJ for 400 nm. Then, the spot density was increased in order to determine the minimum pulse energy required to cut the lens capsule. For 800 nm femtosecond laser, a complete cut could be made with a pulse energy of 0.6 μJ and spot spacing of 1.5 μm laterally and 10 μm vertically. Further increases in spot density didn't allow for lower pulse energies. Using the same process, we found that the 400 nm femtosecond laser was capable of making cuts with only 20 nJ/pulse although it required very dense spot spacing of 0.1 μm laterally and 4 μm vertically. Intriguingly, there were no visible bubbles during cutting and this pulse energy is below the threshold of cavitation bubble formation in water and protein solution as described in section 3.2.

Lens capsule edges imaged with the scanning electron microscopy are shown in Figure 1. Manually torn lens capsule (fig. 1a) has a remarkably smooth edge with fibers that run along the edge of the tear. In contrast, a porcine lens capsule cut using the Catalys (Abbott Medical Optics) laser system (fig. 1b) shows clear laser grooves along the laser direction and perpendicular to the capsule edge. Lens capsule cut with the 800 nm femtosecond laser (fig. 1c) at the minimum pulse energy is qualitatively similar, with clear laser grooves but much closer spot spacing. Unlike the other two laser cuts, 400 nm femtosecond laser can produce very smooth lens capsule edge when operated at or near its minimum pulse energy for cutting. As shown in fig. 1d, the edge is more similar to the manually torn edge in smoothness. However, the orientation of stretch mark or fibers is along the laser direction rather than the capsule edge, confirming that the capsule is split by laser rather than tearing.

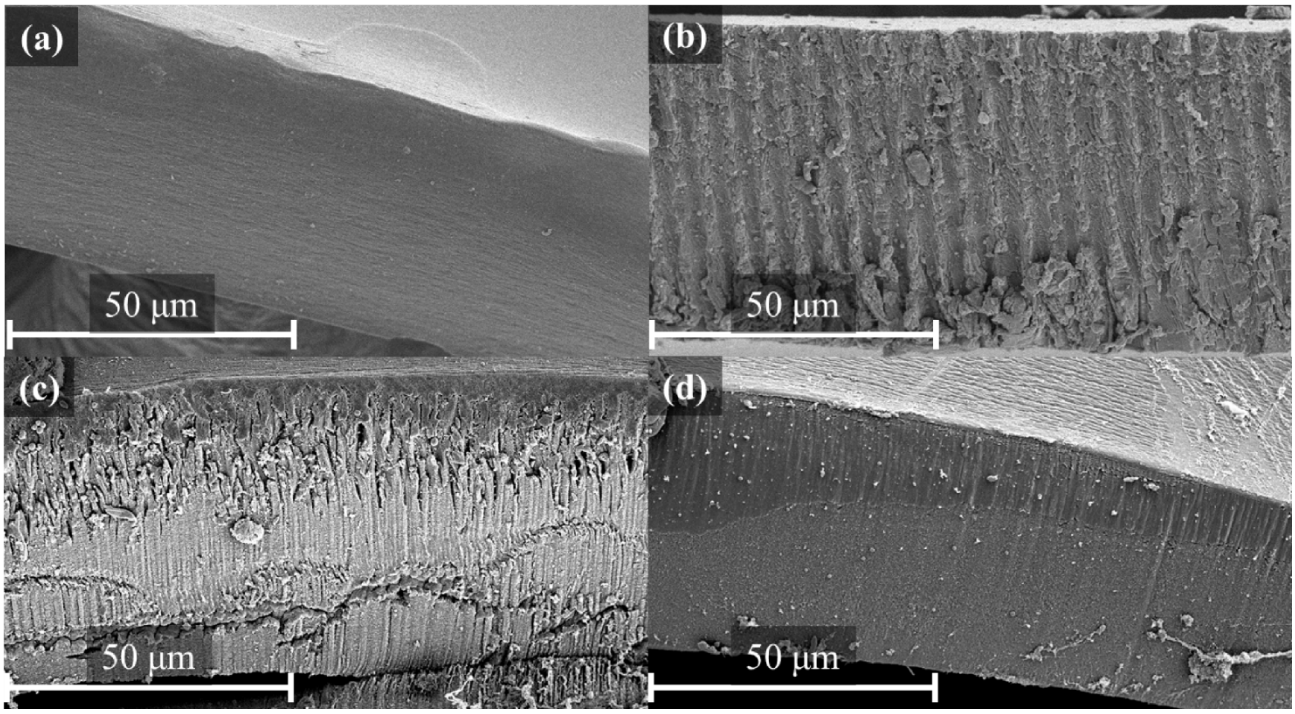

Figure 1. Scanning electron micrographs of porcine lens capsule edge (a) torn with forceps or cut by femtosecond lasers: (b) 10 µJ/pulse, λ = 1030 nm, τ = 400 fs, NA = 0.1, 10 µm spacing vertical and 5µm lateral (c) 0.6 µJ/pulse, λ = 800 nm, τ = 150 fs, NA = 0.1, 10 µm spacing vertical and 1.5 µm lateral (d) 0.02 µJ/pulse, λ = 400 nm, τ = 150 fs, NA = 0.1, 4 µm spacing vertical and 0.1 µm lateral.

3.2 Bubble thresholds in water and in protein solution

Cavitation bubble thresholds were measured with the same laser configurations used in lens capsule cutting, in distilled water and in with different protein concentrations, using a needle pressure transducer. The threshold in distilled water for 800 nm focused at NA 0.1 was 450 nJ, while the threshold for 400 nm was 90 nJ. As shown in figure 2, the addition of BSA up to a concentration of 6 mg/mL lowered the bubble threshold to 81% and 38% of the threshold in distilled water for 800 nm and 400 nm, respectively. After this, further increases of protein concentration increased the bubble threshold.

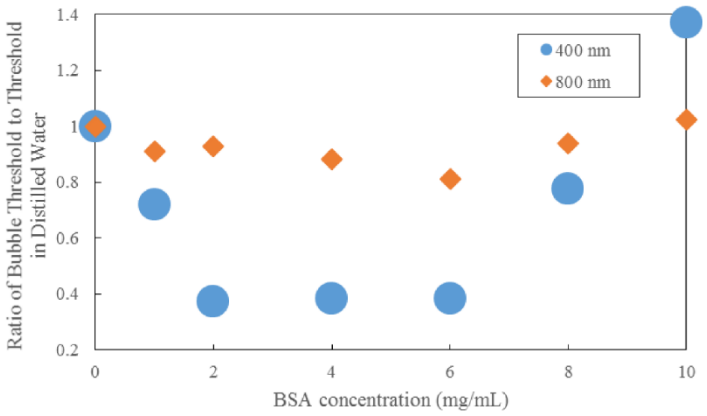

Figure 2. Effect of BSA concentration on bubble threshold. Threshold in distilled water for 400 nm and 800 nm femtosecond laser focused at NA = 0.1 was 90 and 450 nJ, respectively.

3.3 Photodissociation of protein and polypeptide

Gel electrophoresis was used to detect laser-induced breakdown of bovine serum albumin by measuring the intact protein that survives laser irradiation. For 800 nm femtosecond pulses, we use a loosely focused beam that is scanned over a drop of BSA solution (1 mg/mL) at energies at or slightly below the cavitation bubble threshold. The resulting gel in figure 3a shows that 800 nm irradiation, even when repeated 4 times at the cavitation bubble threshold, produces negligible laser-induced protein dissociation as compared to the unirradiated control. The 400 nm femtosecond pulses are capable of inducing protein dissociation at pulse energies below that of cavitation bubbles. As can be seen in Figure 3b, the effect is intensity dependent: unfocused beam produces almost no dissociation at 66% of cavitation bubble threshold, but a focused beam breaks down most of the proteins in solution. This is contrasted with the 193 nm excimer laser where variation of the intensity by almost an order of magnitude, while maintaining constant total energy, does not affect the amount of photodissociation. As shown in Figure 4a, excimer laser breaks down between 50 and 70% of the protein at these settings.

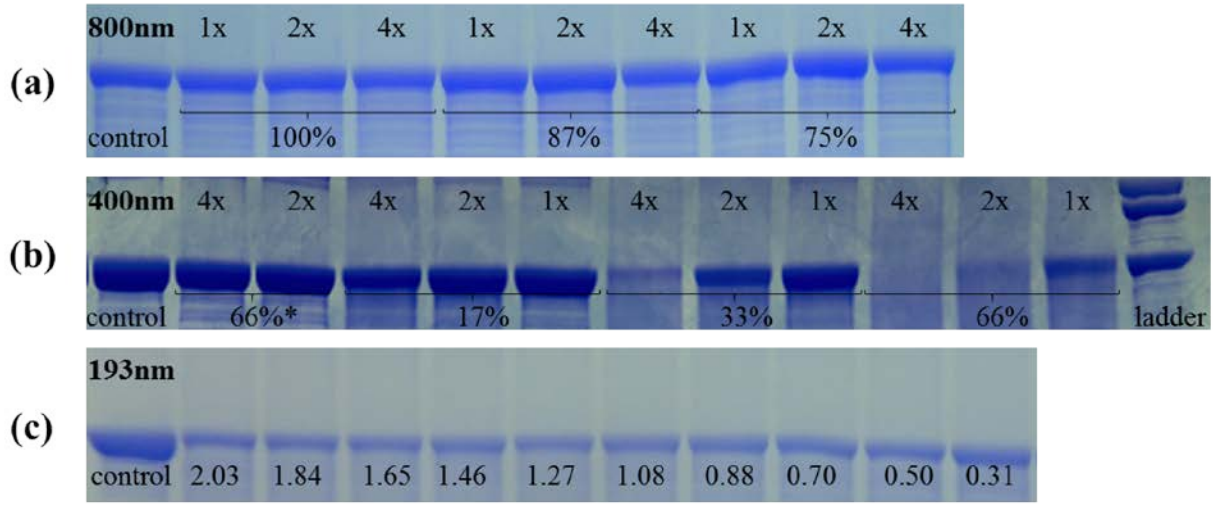

Figure 3. Gel electrophoresis following laser irradiation of bovine serum albumin solution. Stained band represents the remaining amount of full length 66.5 kDa protein (a) 800 nm femtosecond laser scanned over solution with pulse energy as % of bubble threshold and number of repeats (b) 400 nm femtosecond laser scanned over solution with pulse energy as % of bubble threshold and number of repeats. * indicates that focusing lens was removed and beam was unfocused. (c) 193 nm ArF laser with fluence given in mJ/cm^2 and the total number of pulses repeats varied to maintain the constant total delivered energy of 20.6 mJ.

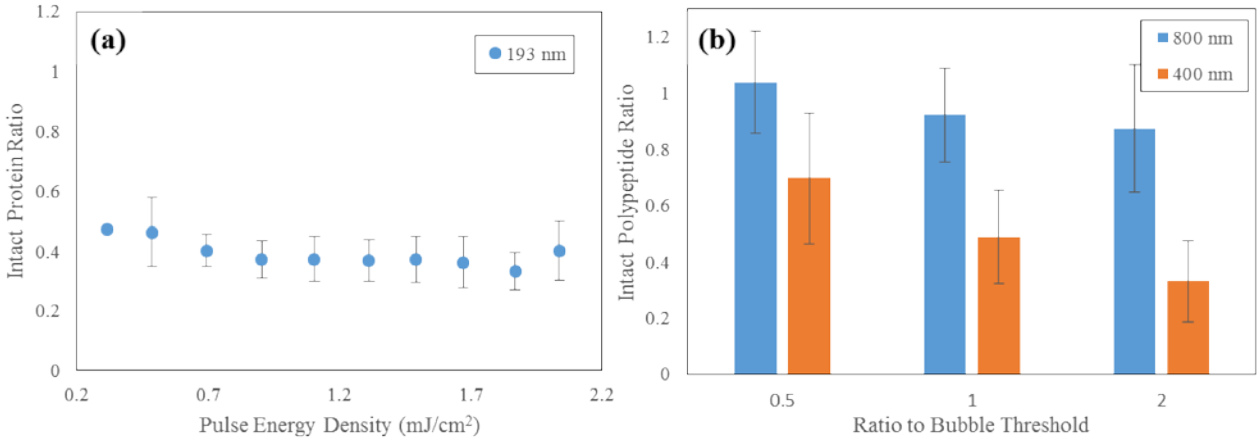

Figure 4. Photodissociation of BSA and polypeptide. (a) Excimer laser breakdown of BSA with number of pulses changing to maintain constant total energy (b) Femtosecond laser breakdown of WHWLQL polypeptide with number of repeats adjusted to maintain constant total energy. The bubble thresholds were was 5 μJ and 20 μJ with 400 and 800 nm lasers in this configuration.

We also used HPLC/MS to measure the amount of intact polypeptide (WHWLQL) after laser-induced photodissociation. At 10 μJ, half the cavitation bubble threshold at 800 nm, laser irradiation shows negligible effect on the polypeptide. Increasing the pulse energy to the cavitation bubble threshold or twice the cavitation bubble threshold produces a slight effect with 92% and 87% of the polypeptide remaining, respectively (fig. 4b). The effect is more robust with 400 nm femtosecond pulses where 10 μJ pulses, twice the cavitation bubble threshold, leaves only 33% of the polypeptide remaining. The effect persists even below the cavitation bubble threshold where 2.5 μJ pulses leave 70% of the polypeptide intact (fig. 4c).

4. DISCUSSION

4.1 Lens capsule cutting

The SEM images of porcine lens capsule provide a detailed look at how 1030 nm, 800 nm, and 400 nm lasers cut tissue. Notably, it shows the potential for improved smoothness of the lens capsule edge when moving to a shorter wavelength. This may be useful for laser capsulotomy since it has been shown that smoother lens capsule edges are more resistant to capsule tears than rougher edges produced by capsulorhexis[11]. Although smaller laser grooves and smoother capsule edge were expected with the shorter wavelength, the ability to cut at energies as low as 20 nJ with minimal laser grooves and no visible bubble production was surprising. Compared to 800 nm at the same focusing angle, we expected an approximately 4-fold reduction in cavitation bubble threshold due to the smaller focal spot size, which we did observe in distilled water (450 vs 90 nJ). However, in lens capsule the minimum cutting energy was 30-fold less for the 400 nm than for 800 nm femtosecond laser.

To understand why 400 nm femtosecond laser could cut lens capsule with surprisingly low pulse energy, we first looked at the effect of protein concentration on the cavitation bubble threshold. A study by Genc et al.[12] showed that biological media such as minimal essential media (MEM) and fetal bovine serum (FBS) reduced the threshold of cavitation bubble formation and plasma luminescence for 532 nm, sub-nanosecond pulses as compared to distilled water. Given that the lens capsule is acellular and composed mainly of collagen, proteoglycans, and glycoproteins[13], we used BSA protein as a simple and soluble substitute for the presence of other molecules in the lens capsule. As expected, the addition of BSA to water decreased the cavitation bubble threshold and the effect was much more pronounced with 400 nm than with 800 nm. However, the minimum bubble threshold was 34 nJ for 400 nm which is still well above the 20 nJ we were able to cut with. A possiblity that a different component of the lens capsule further reduces the cavitation bubble threshold to permit cutting is still being investigated.

4.2 Laser-induced photodissociation

Another possibility for the low pulse energy lens capsule cutting is an alternative mechanism for tissue dissection. Ultrafast lasers have been known to produce photochemical effects without cavitation bubble formation. For instance, near-infrared lasers were reported by Tirlapur et al.[14] as producing reactive oxygen species that produced significant cytotoxicity in mammalian cells. We hypothesized that photochemical interaction between the ultrafast laser pulses and proteins, similar to that which occurs with excimer lasers, could result in dissociation of the proteins and weakening of the lens capsule. Since the lens capsule is under tension, such weakening could be sufficient for creating a cut in the lens capsule. This could also explain why such dense spot spacing was required to complete a cut in the lens capsule.

We explored this hypothesis by first looking for evidence of protein breakdown induced by 400 nm and 800 nm femtosecond laser pulses and compared it to the protein breakdown induced by ArF 193 nm laser pulses. Our gel electrophoresis results support the idea that 400 nm femtosecond pulses can directly breakdown proteins even below the appearance of cavitation bubbles. Unlike excimer laser though, the process is not linear. Thus, it can be confined to a focal volume and is potentially useful for 3D surgical patterning. In contrast, 800 nm femtosecond laser pulses show negligible direct interaction with proteins. The HPLC/MS data shown in figure 4b, indicates that the effect is not merely plasma-mediated photochemistry. In the 800 nm case, there is negligible polypeptide dissociation even at twice the cavitation bubble threshold, where a significant plasma is generated. For 400 nm, the effect is more robust and present even at half the cavitation bubble threshold suggesting a direct interaction between laser and polypeptides even without plasma.

5. CONCLUSION

Comparison of the lens capsule cutting with femtosecond lasers at visible (400nm) and near-IR (800nm) wavelengths, demonstrates that visible lasers are capable of remarkably smooth cuts below the apparent cavitation bubble threshold. Visible fs lasers induced significant photodissociation of proteins and polypeptides, while the infrared laser did not.

ACKNOWLEDGEMENTS

Funding was provided by the U.S. Air Force Office of Scientific Research and the Stanford Photonics Research Center.

REFERENCES

[1] Trokel, S.L., Srinivasan, R., and Braren, B., “Excimer laser surgery of the cornea.,” American journal of ophthalmology 96(6), 710–715 (1983).
[2] Ratkay-Traub, I., Ferincz, I.E., Juhasz, T., Kurtz, R.M., and Krueger, R.R., “First clinical results with the femtosecond neodynium-glass laser in refractive surgery.,” Journal of refractive surgery (Thorofare, N.J. : 1995) 19(2), 94–103 (2003).
[3] Shousha, M.A., Yoo, S.H., Kymionis, G.D., Ide, T., Feuer, W., Karp, C.L., O’Brien, T.P., Culbertson, W.W., and Alfonso, E., “Long-term results of femtosecond laser-assisted sutureless anterior lamellar keratoplasty.,” Ophthalmology 118(2), 315–23 (2011).
[4] Nagy, Z., Takacs, A., Filkorn, T., and Sarayba, M., “Initial clinical evaluation of an intraocular femtosecond laser in cataract surgery,” Journal of Refractive Surgery 25(12), 1053–60 (2009).
[5] Palanker, D. V, Blumenkranz, M.S., Andersen, D., Wiltberger, M., Marcellino, G., Gooding, P., Angeley, D., Schuele, G., Woodley, B., et al., “Femtosecond laser-assisted cataract surgery with integrated optical coherence tomography,” Science Translational Medicine 2(58), 58ra85 (2010).
[6] Vogel, A., and Venugopalan, V., “Mechanisms of pulsed laser ablation of biological tissues.,” Chemical reviews 103(2), 577–644 (2003).
[7] Vogel, A., Linz, N., Freidank, S., Liang, X., and Phipps, C., “Controlled Nonlinear Energy Deposition In Transparent Materials: Experiments And Theory,” in AIP Conf. Proc. 51, 51–55 (2010).
[8] Trost, A., Schrödl, F., Strohmaier, C. a, Bogner, B., Runge, C., Kaser-Eichberger, A., Krefft, K.A., Vogel, A., Linz, N., et al., “A new nanosecond UV-laser at 355 nm: early results of corneal flap cutting in a rabbit model.,” Investigative ophthalmology & visual science 54(13), 7854–64 (2013).

[9] Crotti, C., Deloison, F., Alahyane, F., Aptel, F., Kowalczuk, L., Legeais, J.-M., Peyrot, D. a, Savoldelli, M., and Plamann, K., "Wavelength optimization in femtosecond laser corneal surgery.," Investigative ophthalmology & visual science 54(5), 3340–9 (2013).
[10] Xu, L., Knox, W.H., DeMagistris, M., Wang, N., and Huxlin, K.R., "Noninvasive Intratissue Refractive Index Shaping (IRIS) of the Cornea with Blue Femtosecond Laser Light," Investigative Ophthalmology & Visual Science 52(11), 8148–8155 (2011).
[11] Andreo, L.K., Wilson, M.E., and Apple, D.J., "Elastic properties and scanning electron microscopic appearance of manual continuous curvilinear capsulorhexis and vitrectorhexis in an animal model of pediatric cataract," Journal of Cataract & Refractive Surgery 25(4), 534–539 (1999).
[12] Genc, S.L., Ma, H., and Venugopalan, V., "Low-density plasma formation in aqueous biological media using sub-nanosecond laser pulses," Applied Physics Letters 105(6), 063701 (2014).
[13] Danysh, B.P., and Duncan, M.K., "The lens capsule.," Experimental eye research 88(2), 151–64 (2009).
[14] Tirlapur, U.K., König, K., Peuckert, C., Krieg, R., and Halbhuber, K.J., "Femtosecond near-infrared laser pulses elicit generation of reactive oxygen species in mammalian cells leading to apoptosis-like death.," Experimental cell research 263(1), 88–97 (2001).